

Multilayered solar interface dynamos: from a Cartesian kinematic dynamo to a spherical dynamic dynamo

Kit H. Chan¹, Xinhao Liao²
and Keke Zhang³

¹Department of Mathematics, The University of Hong Kong, Pokfulam, Hong Kong
email:mkhchan@hku.hk

²Shanghai Astronomical Observatory, Shanghai 200030, China
email:xhliao@shao.ac.cn

³Center for Geophysical & Astrophysical Fluid Dynamics, University of Exeter, UK
email:kzhang@ex.ac.uk

Abstract.

The existence of the solar tachocline, a thin differentially rotating layer at the base of the convection zone which is inferred from helioseismology, leads to the concept of an interface dynamo. The tachocline is magnetically coupled to the radiative interior and the overlying convection zone. A multilayered interface dynamo is required to describe the dynamo process involved. We first discuss a two-dimensional multilayered interface dynamo model in cartesian geometry consisting of four horizontal layers with different magnetic diffusivities magnetically coupled by the three sets of interface matching conditions for the generated magnetic field. Exact solutions of the coupled dynamo system are obtained in this model. We then discuss a fully three-dimensional and multi-layered spherical dynamic interface dynamo using a finite element method based on the three-dimensional tetrahedralization of the whole spherical system. The spherical dynamic interface dynamo also consists of four magnetically coupled zones. In the convection zone, the fully three-dimensional dynamic feedback of Lorentz forces is taken into account. It is shown that the dynamo is characterized by a strong toroidal magnetic field, selects dipolar symmetry and propagates equatorward.

Keywords. Solar magnetic fields, interface dynamos, dynamics

1. Introduction

The Sun is a magnetic, slowly rotating star. The most important feature of the solar magnetic field is the dark regions on its surface, known as sunspots. The sunspots have been observed systematically over the past two thousand years, first by Chinese astronomers and then by western astronomers with the help of telescopes. Modern observations together with historical records show that the Sun's magnetic field has undergone nearly periodic variations with the period about 22 years, except a suspension at the end of the 17th century (the Maunder minimum), over the past several hundred years (see for example, Hoyt and Schatten, 1997).

The globally systematic, ordered variation of the solar magnetic field such as the 22-year sunspot cycle can be only explained by the dynamo process associated with the operation of non-turbulent, large-scale, regular flow that controls the solar dynamo. Recent systematic helioseismic measurements suggest the existence of the tachocline at the base of the convection zone, a strong radial shear in the solar differential rotation (see for example, Brown *et al.*, 1989; Spiegel & Zahn, 1992; Schou *et al.*, 1998). This

leads to the first solar interface dynamo model, with two layers, in cartesian geometry by Parker (1993) in which the generation of a weak poloidal magnetic field and a strong toroidal magnetic field takes place in separate fluid regions with discontinuous magnetic diffusivities across their interface. A number of solar dynamo models in simple Cartesian geometry have been then constructed to explain the main features of the observed solar magnetic activity. MacGregor & Charbonneau (1997) considered a different interface dynamo in which the shear flow and α -effects are spatially localized in the form of delta-functions on either side of the interface. Because the shear flow and α -effects are spatially separated, the effect of magnetic diffusion plays a more important role compared to the model with a uniformly distributed shear and alpha. The effect of the radiative solar interior on the interface dynamo was investigated by Zhang *et al.* (2004). By introducing the action of the Lorentz force using the Malkus-Proctor mechanism, Tobias (1997) investigated the nonlinear modulation of Parker's interface dynamo capable of producing the long-term modulation of the basic solar magnetic cycle and recurrent grand minima (see also Brandenburg *et al.*, 1989; Ponty *et al.*, 2001). Cartesian geometry is mainly adopted for understanding the fundamental dynamo processes because an analytical method can be used, offering important insights into the physics of the solar dynamo in the parameter regime where direct numerical simulations in spherical geometry are difficult.

Parker's cartesian interface dynamo has also been extended to spherical geometry (see, for example, Charbonneau & MacGregor, 1997; Markiel & Thomas, 1999; Dikpati & Charbonneau, 1999; Zhang *et al.*, 2003; Bushby, 2003; Chan *et al.*, 2004). Spherical interface dynamos usually employ a solar-like internal differential rotation profile obtained from the helioseismic inversion. As far as magnetic field generation is concerned, the radial shear in the tachocline plays a much more significant role than the latitudinal variation in the differential rotation. In particular, Markiel & Thomas (1999) demonstrated that the magnetic boundary condition can play a critical role in determining the key features of an interface dynamo and that the radial shear in the tachocline dominates the process of magnetic field generation even though the latitudinal shear is present. Without the effect of the tachocline, the conventional nonlinear α^2 dynamo is usually stationary and equatorially symmetric or antisymmetric even though numerical simulations are fully three-dimensional and time-dependent. In a fully three-dimensional and multilayered spherical kinematic interface dynamo, Zhang *et al.* (2003) showed that the action of the steady tachocline always gives rise to an oscillatory dynamo with a period of about two magnetic diffusion units and the spherical kinematic interface dynamo selects dipolar symmetry and propagates equatorward with the strength of the generated toroidal magnetic field dramatically amplified by the effect of the tachocline.

In this review article, we shall first discuss a multilayered two-dimensional kinematic interface dynamo in which the exact solution can be obtained, which is given in Section 2. This is followed by a fully three-dimensional and multilayered spherical dynamic interface dynamo using a finite element method based on the three-dimensional tetrahedralization of the whole spherical system presented in Section 3. Section 4 closes the paper with a summary and some remarks.

2. A Multilayered Cartesian Interface Dynamo

We first consider a multilayered cartesian interface dynamo in which the alpha-effect and velocity shear are uniformly distributed throughout the corresponding regions. In this case, the mathematical analysis is analytically tractable, while retaining the essential

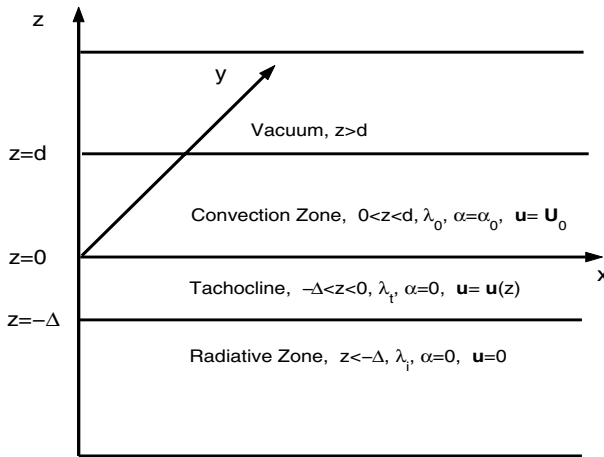


Figure 1. Schematic geometry of the two-dimensional multi-layered interface dynamo with four regions.

physics of the problem. The model, depicted schematically in Figure 1, consists of four different regions (see Zhang *et al.*, 2004).

The radiative zone in $-\Delta > z > -\infty$ has constant magnetic diffusivity λ_i . The magnetic field \mathbf{B}_i there is governed by the equations

$$\frac{\partial \mathbf{B}_i}{\partial t} + \lambda_i \nabla \times \nabla \times \mathbf{B}_i = 0, \quad -\Delta > z > -\infty, \tag{2.1}$$

$$\nabla \cdot \mathbf{B}_i = 0, \quad -\Delta > z > -\infty. \tag{2.2}$$

There is no flow in the radiative zone so the magnetic field \mathbf{B}_i cannot be generated in this region. But \mathbf{B}_i is usually non-zero because of the magnetic diffusion and the magnetic coupling with the tachocline. This process could control the characteristics of the dynamo solution in the whole system. Above the radiative zone is the tachocline in $-\Delta < z < 0$, a region of strong differential rotation with a flow velocity given by $\mathbf{u}(z)$. The differential rotation shears the weak poloidal magnetic field that is generated in the convection zone and penetrates into the tachocline. This amplification process in the tachocline is described by the equations

$$\frac{\partial \mathbf{B}_t}{\partial t} = \nabla \times (\mathbf{u} \times \mathbf{B}_t) - \lambda_t \nabla \times \nabla \times \mathbf{B}_t, \quad -\Delta < z < 0, \tag{2.3}$$

$$\nabla \cdot \mathbf{B}_t = 0, \quad -\Delta < z < 0, \tag{2.4}$$

where λ_t is the magnetic diffusivity in the tachocline and $\mathbf{u}(z)$ is given by

$$\mathbf{u}(z) = \mathbf{U}_0 u(z) = U \mathbf{e}_y u(z), \quad -\Delta < z < 0, \tag{2.5}$$

where \mathbf{U}_0 is a constant vector, U is constant and $u(z)$ satisfies

$$u(z) = 0, \quad z = -\Delta; \quad u(z) = 1, \quad z = 0. \tag{2.6}$$

The cartesian coordinate system (x, y, z) with unit vectors $(\mathbf{e}_x, \mathbf{e}_y, \mathbf{e}_z)$ is oriented in such a way that the directions of increasing x, y and z are along the directions of the spherical polar coordinates θ, ϕ and r , respectively. In this case, the shear flow $\mathbf{u}(z)$ is in the azimuthal direction (y -direction).

Fully turbulent convection is assumed in the region $0 < z < d$ with eddy magnetic diffusivity λ_o and magnetic field \mathbf{B}_o generated by an α -effect which is described by

$$\frac{\partial \mathbf{B}_o}{\partial t} = \nabla \times (\mathbf{U}_0 \times \mathbf{B}_o) + \nabla \times (\alpha_o \mathbf{B}_o) - \lambda_o \nabla \times \nabla \times \mathbf{B}_o, \quad 0 < z < d, \quad (2.7)$$

$$\nabla \cdot \mathbf{B}_o = 0, \quad 0 < z < d, \quad (2.8)$$

where α_o is assumed to be a constant, positive parameter. The effect of the weak differential rotation in the convection zone is neglected by assuming that \mathbf{U}_0 is uniform. The velocity is continuous across the convection-tachocline interface as indicated by (2.5) and (2.6) while the velocity shear (du/dz) is discontinuous. The upper exterior to the convection zone, $d < z < \infty$, is assumed to be electrically insulating and its magnetic field \mathbf{B}_e is governed by

$$\nabla \times \mathbf{B}_e = 0, \quad \nabla \cdot \mathbf{B}_e = 0, \quad d < z < \infty. \quad (2.9)$$

We nondimensionalize length by the thickness of the convection zone d and time by the magnetic diffusion time d^2/λ_o of the convection zone. The resulting four sets of dimensionless equations for the four zones (all variables in the rest are non-dimensional) are

$$\frac{\partial \mathbf{B}_i}{\partial t} = -\beta_i \nabla \times \nabla \times \mathbf{B}_i, \quad \nabla \cdot \mathbf{B}_i = 0, \quad -\infty < z < -\Delta/d; \quad (2.10)$$

$$\frac{\partial \mathbf{B}_t}{\partial t} = R_\omega \nabla \times (\mathbf{u} \times \mathbf{B}_t) - \beta_t \nabla \times \nabla \times \mathbf{B}_t, \quad -\Delta/d < z < 0, \quad (2.11)$$

$$\nabla \cdot \mathbf{B}_t = 0, \quad -\Delta/d < z < 0; \quad (2.12)$$

$$\frac{\partial \mathbf{B}_o}{\partial t} = R_\omega \nabla \times (\mathbf{e}_y \times \mathbf{B}_o) + R_\alpha \nabla \times \mathbf{B}_o - \nabla \times \nabla \times \mathbf{B}_o, \quad 0 < z < 1, \quad (2.13)$$

$$\nabla \cdot \mathbf{B}_o = 0, \quad 0 < z < 1; \quad (2.14)$$

$$\nabla \times \mathbf{B}_e = 0, \quad \nabla \cdot \mathbf{B}_e = 0, \quad 1 < z < \infty. \quad (2.15)$$

There are four non-dimensional quantities that characterize the multilayered interface dynamo: the magnetic diffusivity ratios β_i, β_t , the magnetic alpha Reynolds number R_α and the magnetic omega Reynolds number R_ω , which are defined by

$$\beta_i = \frac{\lambda_i}{\lambda_o}, \quad \beta_t = \frac{\lambda_t}{\lambda_o}, \quad R_\alpha = \frac{d\alpha_o}{\lambda_o}, \quad R_\omega = \frac{dU}{\lambda_o}. \quad (2.16)$$

The governing equations for the four different zones are solved subject to a number of matching and boundary conditions. At the three interfaces of the four zones, $z = -\Delta/d, 0$ and 1 , all components of the magnetic field and the tangential component of the electrical field must be continuous. These conditions yield

$$\mathbf{B}_i = \mathbf{B}_t \text{ at } z = -\frac{\Delta}{d}; \quad (2.17)$$

$$\mathbf{e}_z \times (\beta_i \nabla \times \mathbf{B}_i) = \mathbf{e}_z \times (\beta_t \nabla \times \mathbf{B}_t - R_\omega \mathbf{S}_t) \text{ at } z = -\frac{\Delta}{d}; \quad (2.18)$$

$$\mathbf{B}_t = \mathbf{B}_o \text{ at } z = 0; \quad (2.19)$$

$$\mathbf{e}_z \times (\beta_t \nabla \times \mathbf{B}_t - R_\omega \mathbf{S}_t) = \mathbf{e}_z \times [\nabla \times \mathbf{B}_o - R_\alpha \mathbf{B}_o - R_\omega \mathbf{e}_y \times \mathbf{B}_o] \text{ at } z = 0; \quad (2.20)$$

$$\mathbf{B}_e = \mathbf{B}_o \text{ at } z = 1, \quad (2.21)$$

where $\mathbf{S}_t = \mathbf{u}_t \times \mathbf{B}_t$. Additionally, there are no sources at infinity, which implies

$$\mathbf{B}_i \rightarrow 0, \quad \text{as } z \rightarrow -\infty; \quad \mathbf{B}_e \rightarrow 0, \quad \text{as } z \rightarrow +\infty. \quad (2.22)$$

Equations (2.10-2.15) together with the matching conditions (2.17-2.21) and boundary conditions (2.22), define a linear, multilayered kinematic interface dynamo problem. For given parameters of the model such as R_α and R_ω , exact solutions of the interface dynamo are sought by first finding the dispersion relation and then the solutions representing horizontally propagating dynamo waves.

The generated mean magnetic field is assumed to be independent of y . It is thus mathematically convenient to express a magnetic field in terms of its azimuthal field in the y -direction and a vector potential (Parker, 1993) by denoting

$$\begin{aligned} \mathbf{B}_i &= B_i(x, z, t)\mathbf{e}_y + \nabla \times [A_i(x, z, t)\mathbf{e}_y] \text{ in } -\infty < z < -\Delta/d; \\ \mathbf{B}_t &= B_t(x, z, t)\mathbf{e}_y + \nabla \times [A_t(x, z, t)\mathbf{e}_y] \text{ in } -\Delta/d < z < 0; \\ \mathbf{B}_o &= B_o(x, z, t)\mathbf{e}_y + \nabla \times [A_o(x, z, t)\mathbf{e}_y] \text{ in } 0 < z < 1; \\ \mathbf{B}_e &= B_e(x, z, t)\mathbf{e}_y + \nabla \times [A_e(x, z, t)\mathbf{e}_y] \text{ in } 1 < z < \infty. \end{aligned} \quad (2.23)$$

They automatically satisfy the divergence-free condition. Based on expression (2.23), vector dynamo equations can be rewritten as two scalar equations for the toroidal component and the poloidal component.

Not all the matching conditions at the three interfaces derived from (2.17-2.21) are independent. There are four independent matching conditions required at the core and tachocline interface

$$B_i = B_t, \quad A_i = A_t \text{ at } z = -\Delta/d; \quad (2.24)$$

$$\frac{\partial A_i}{\partial z} = \frac{\partial A_t}{\partial z}, \quad \beta_i \frac{\partial B_i}{\partial z} = \beta_t \frac{\partial B_t}{\partial z} + R_\omega u \frac{\partial A_t}{\partial x} \text{ at } z = -\Delta/d. \quad (2.25)$$

The two vector matching conditions at $z = -\Delta/d$ give a total of four independent conditions. Similarly, there are four independent conditions required at the interface between the tachocline and the convection zone

$$B_t = B_o, \quad A_t = A_o \text{ at } z = 0; \quad (2.26)$$

$$\beta_i \frac{\partial B_t}{\partial z} = \frac{\partial B_o}{\partial z}, \quad \frac{\partial A_t}{\partial z} = \frac{\partial A_o}{\partial z} \text{ at } z = 0. \quad (2.27)$$

The three conditions required at the outer surface of the convection zone are simply

$$B_o = 0, \quad A_o = A_e, \quad \frac{\partial A_o}{\partial z} = \frac{\partial A_e}{\partial z} \text{ at } z = 1. \quad (2.28)$$

Furthermore, the boundary conditions at infinity requires

$$B_i = 0, \quad A_i = 0, \text{ at } z = -\infty; \quad (2.29)$$

$$A_e = 0, \text{ at } z = +\infty. \quad (2.30)$$

Altogether there are eleven matching and boundary conditions. The linear dynamo equations allow us to consider a horizontally propagating wave solution in the form

$$[A_i, B_i, A_t, B_t, A_o, B_o, A_e](x, z, t) = [A_i, B_i, A_t, B_t, A_o, B_o, A_e](z)e^{i(kx + \omega t) + \sigma t}, \quad (2.31)$$

where $i = \sqrt{-1}$, ω is the real frequency of a wave, k is the horizontal wavenumber and σ is the real growth rate. When $k > 0$ and $\omega < 0$, the dynamo wave propagates toward the positive x -direction (toward the equator in spherical geometry). Using the wave-type solution in the form (2.31), the z -dependent portion of a dynamo solution for the toroidal and poloidal components, such as $A_i(z)$ and $B_i(z)$, can be readily derived. In the radiative layer, a solution for the magnetic field can be written as

$$B_i(z) = \hat{B}_i e^{z(S_i - iQ_i)}, \text{ in } -\infty < z < \Delta/d; \quad (2.32)$$

$$A_i(z) = \hat{A}_i e^{z(S_i - iQ_i)}, \text{ in } -\infty < z < \Delta/d, \tag{2.33}$$

where \hat{B}_i and \hat{A}_i are the complex amplitude to be determined, and S_i and Q_i are real, positive and defined by

$$S_i = \frac{1}{\sqrt{2}} \left\{ + \left(k^2 + \frac{\sigma}{\beta_i} \right) + \left[\left(k^2 + \frac{\sigma}{\beta_i} \right)^2 + \left(\frac{\omega}{\beta_i} \right)^2 \right]^{1/2} \right\}^{1/2},$$

$$Q_i = \frac{1}{\sqrt{2}} \left\{ - \left(k^2 + \frac{\sigma}{\beta_i} \right) + \left[\left(k^2 + \frac{\sigma}{\beta_i} \right)^2 + \left(\frac{\omega}{\beta_i} \right)^2 \right]^{1/2} \right\}^{1/2}.$$

In the tachocline, we have to assume the profile of the vertical shear flow $u(z)$. The simplest profile is the uniform shear given by

$$u(z) = \frac{d}{\Delta} \left(z + \frac{\Delta}{d} \right), \quad \frac{\partial u}{\partial z} = \frac{d}{\Delta}, \quad -\Delta/d < z < 0. \tag{2.34}$$

In this case, a general solution in the region $-\Delta/d < z < 0$ is given by

$$B_t(z) = \left[\hat{B}_t^+ + \frac{\hat{A}_t^+ i \hat{R}_\omega k z}{2\beta_t(S_t - iQ_t)} \right] e^{z(S_t - iQ_t)} + \left[\hat{B}_t^- - \frac{\hat{A}_t^- i \hat{R}_\omega k z}{2\beta_t(S_t - iQ_t)} \right] e^{-z(S_t - iQ_t)},$$

$$A_t(z) = \hat{A}_t^+ e^{z(S_t - iQ_t)} + \hat{A}_t^- e^{-z(S_t - iQ_t)}, \tag{2.35}$$

where $\hat{B}_t^+, \hat{B}_t^-, \hat{A}_t^+$ and \hat{A}_t^- are the complex amplitude of the dynamo solution to be determined, \hat{R}_ω is defined as $\hat{R}_\omega = R_\omega/(d\Delta)$ and S_t and Q_t are real, positive and defined by

$$S_t = \frac{1}{\sqrt{2}} \left\{ + \left(k^2 + \frac{\sigma}{\beta_t} \right) + \left[\left(k^2 + \frac{\sigma}{\beta_t} \right)^2 + \left(\frac{\omega}{\beta_t} \right)^2 \right]^{1/2} \right\}^{1/2},$$

$$Q_t = \frac{1}{\sqrt{2}} \left\{ - \left(k^2 + \frac{\sigma}{\beta_t} \right) + \left[\left(k^2 + \frac{\sigma}{\beta_t} \right)^2 + \left(\frac{\omega}{\beta_t} \right)^2 \right]^{1/2} \right\}^{1/2}.$$

For the convection zone in the region $0 < z < 1$, a general solution is of the form

$$A_o(z) = \left[\hat{A}_o^+ + \frac{B_o^+ R_\alpha z}{2(S_o - iQ_o)} \right] e^{z(S_o - iQ_o)} + \left[\hat{A}_o^- - \frac{B_o^- R_\alpha z}{2(S_o - iQ_o)} \hat{B}_o^- \right] e^{-z(S_o - iQ_o)},$$

$$B_o(z) = \hat{B}_o^+ e^{z(S_o - iQ_o)} + \hat{B}_o^- e^{-z(S_o - iQ_o)}, \tag{2.36}$$

where $\hat{B}_o^+, \hat{B}_o^-, \hat{A}_o^+$ and \hat{A}_o^- are the complex amplitude of the solution to be determined and, S_o and Q_o are real, positive and defined by

$$S_o = \frac{1}{\sqrt{2}} \left\{ + (k^2 + \sigma) + \left[(k^2 + \sigma)^2 + \omega^2 \right]^{1/2} \right\}^{1/2},$$

$$Q_o = \frac{1}{\sqrt{2}} \left\{ - (k^2 + \sigma) + \left[(k^2 + \sigma)^2 + \omega^2 \right]^{1/2} \right\}^{1/2}.$$

For the vacuum exterior in the region $1 < z < \infty$, a general solution is simply

$$A_e(z) = \hat{A}_e e^{-kz}, \tag{2.37}$$

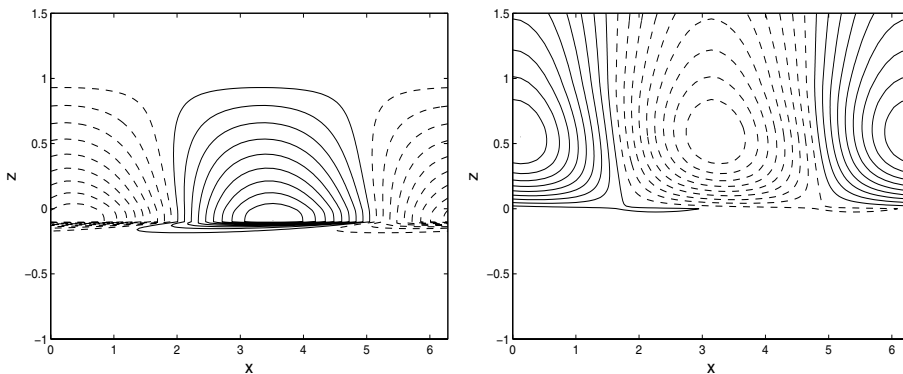


Figure 2. Contours of the azimuthal field (B) (left panel) and the field lines of poloidal field (A) (right panel) in the x - z plane for $\hat{R}_\omega = 300$ and $R_\alpha = 30$ for $\beta_i = 0.001, \beta_t = 1$. Solid contours indicate the field with $B > 0$ or $A > 0$ and dashed contours correspond to $B < 0$ or $A < 0$.

where \hat{A}_e is the complex amplitude of the solution to be determined by the matching conditions.

Substitution of (2.32)-(2.37) into the eleven interface matching conditions, yields the eleven linear complex equations

$$\begin{aligned}
 & -\hat{B}_i e^{-c_i \Delta/d} + \left(\hat{B}_t^+ - \frac{\hat{A}_t^+ i \hat{R}_\omega k \Delta}{2\beta_t d C_t} \right) e^{-c_t \Delta/d} + \left(\hat{B}_t^- + \frac{\hat{A}_t^- i \hat{R}_\omega k \Delta}{2\beta_t d C_t} \right) e^{c_t \Delta/d} = 0, \\
 & -\hat{A}_i e^{-c_i \Delta/d} + \hat{A}_t^+ e^{-c_t \Delta/d} + \hat{A}_t^- e^{c_t \Delta/d} = 0, \\
 & -\hat{A}_i C_i e^{-c_i \Delta/d} + C_t \left(\hat{A}_t^+ e^{-c_t \Delta/d} - \hat{A}_t^- e^{c_t \Delta/d} \right) = 0, \\
 & -\beta_i C_i \hat{B}_i e^{-c_i \Delta/d} + \beta_t \left(C_t \hat{B}_t^+ + \frac{\hat{A}_t^+ \hat{R}_\omega \mathcal{D}^+}{2\beta_t} \right) e^{-c_t \Delta/d} - \beta_t \left(C_t \hat{B}_t^- + \frac{\hat{A}_t^- \hat{R}_\omega \mathcal{D}^-}{2\beta_t} \right) e^{c_t \Delta/d} = 0, \\
 & \hat{B}_t^+ + \hat{B}_t^- - \hat{B}_o^+ - \hat{B}_o^- = 0, \\
 & \hat{A}_t^+ + \hat{A}_t^- - \hat{A}_o^+ - \hat{A}_o^- = 0, \\
 & -C_t \left(\hat{A}_t^+ - \hat{A}_t^- \right) + C_o \left(\hat{A}_o^+ - \hat{A}_o^- \right) + \frac{R_\alpha}{2C_o} \left(\hat{B}_o^+ - \hat{B}_o^- \right) = 0, \\
 & \beta_t C_t \left[\hat{B}_t^+ - \hat{B}_t^- + \frac{i \hat{R}_\omega k}{2\beta_t C_t^2} \left(\hat{A}_t^+ - \hat{A}_t^- \right) \right] - C_o \left(\hat{B}_o^+ - \hat{B}_o^- \right) = 0, \\
 & \hat{B}_o^+ e^{c_o} + \hat{B}_o^- e^{-c_o} = 0, \\
 & \left(\hat{A}_o^+ + \frac{\hat{B}_o^+ R_\alpha}{2C_o} \right) e^{c_o} + \left(\hat{A}_o^- - \frac{\hat{B}_o^- R_\alpha}{2C_o} \right) e^{-c_o} - \hat{A}_e e^{-k} = 0, \\
 & \left[C_o \hat{A}_o^+ + \frac{\hat{B}_o^+ R_\alpha}{2} \left(\frac{1}{C_o} + 1 \right) \right] e^{c_o} - \left[C_o \hat{A}_o^- + \frac{\hat{B}_o^- R_\alpha}{2} \left(\frac{1}{C_o} - 1 \right) \right] e^{-c_o} + \hat{A}_e k e^{-k} = 0,
 \end{aligned}$$

where $C_i, C_t, C_o, \mathcal{D}^+$ and \mathcal{D}^- are complex and defined as

$$C_i = S_i - iQ_i, \quad C_t = S_t - iQ_t, \quad C_o = S_o - iQ_o, \quad \mathcal{D}^+ = ik \left(-\frac{\Delta}{d} + \frac{1}{C_t} \right), \quad \mathcal{D}^- = ik \left(\frac{\Delta}{d} + \frac{1}{C_t} \right).$$

In order that the above complex equations have non-trivial solutions, its complex deter-

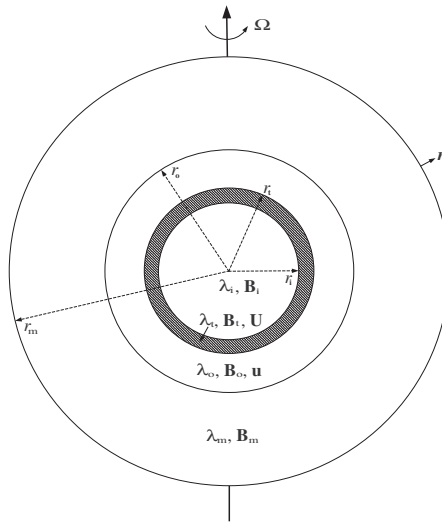


Figure 3. Geometry of the three-dimensional, four-zone, dynamic interface dynamo model: $0 < r \leq r_i$, the uniformly rotating, electrically conducting core with magnetic diffusivity λ_i ; $r_i \leq r \leq r_t$, the differentially rotating tachocline with magnetic diffusivity λ_t ; $r_t \leq r \leq r_o$, the convection zone with magnetic diffusivity λ_o ; and $r > r_o$, the exterior with large magnetic diffusivity λ_e .

minant must vanish,

$$\text{Det}|\mathcal{M}(R_\alpha, R_\omega, k, \beta_i, \beta_t, \omega, \sigma)| = 0. \tag{2.38}$$

For a given set of parameters, $(R_\alpha, R_\omega, k, \beta_i, \beta_t)$, the real and imaginary parts of (2.38) give two equations for ω and σ . After solving the dispersion relation (2.38) and then substituting $(R_\alpha, R_\omega, k, \beta_i, \beta_t, \omega, \sigma)$ into the above eleven complex equations, we solve for $(\hat{B}_i, \hat{A}_i, \hat{B}_t^+, \hat{B}_t^-, \hat{A}_t^+, \hat{A}_t^-, \hat{B}_o^+, \hat{B}_o^-, \hat{A}_o^+, \hat{A}_o^-, \hat{A}_e)$, give the exact solution for a multilayered interface dynamo in the whole domain $-\infty < z < \infty$.

Dispersion relation (2.38) and the corresponding exact dynamo solution have been calculated for a given set of the parameters of the problem. A typical dynamo solution is shown in Figure 2 describing the azimuthal field and the field lines of poloidal field in the x - z plane with $\hat{R}_\omega = 300$ and $R_\alpha = 30$ for $\beta_i = 0.001, \beta_t = 1$. The dynamo wave propagates toward the positive x -direction ($k > 0, \omega < 0$) while the strong toroidal field generated concentrates in the region of the thin tachocline. But the poloidal field generated in the convection zone is mainly concentrated in the convection zone since the strong shear in the tachocline prevents the poloidal field from penetrating into the deep radiative layer.

3. A Multilayered Spherical Dynamic Interface Dynamo

We now consider a much more complicated multilayered dynamo: a three-dimensional, spherical, dynamic interface dynamo consisting of four different zones as illustrated in Figure 3. The inner radiative sphere, $0 < r < r_i$, with constant magnetic diffusivity λ_i , is assumed to rotate uniformly with the angular velocity Ω . In comparison to the kinematic dynamo problem, the dynamic interface dynamo requires not only an additional equation of motion but also additional physical parameters, such as the Taylor number Ta , pertaining to the dynamic problem in rotating fluid systems. An element-by-element (EBE) finite element method capable of taking the full advantage of modern massively parallel

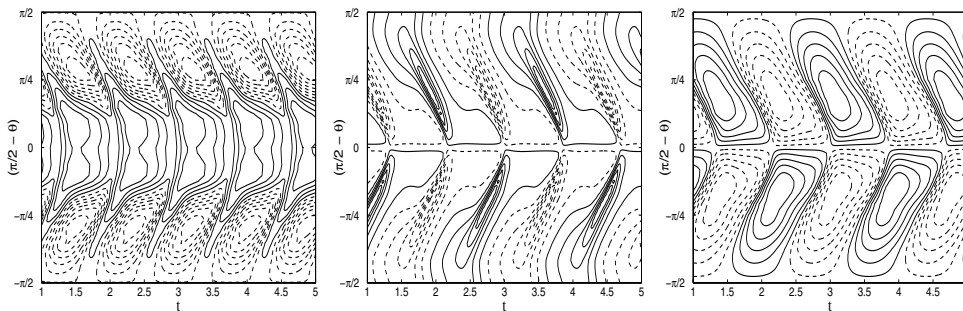


Figure 4. The butterfly-type diagram for the azimuthal flow u_ϕ (top panel) and the radial magnetic field B_r (middle panel) at the middle surface of the convection zone, and the azimuthal magnetic field B_ϕ (bottom panel) at the base of the convection zone for $R_m = 200$. The dynamic dynamo solution is axisymmetric.

computers is employed in the numerical simulation of three-dimensional, spherical, dynamic interface dynamos. The EBE finite-element code has been carefully compared with the well-known benchmark dynamo using spectral methods, showing a satisfactory agreement between two fundamentally different models (Chan et al., 2007).

By scaling the equations with length by the thickness of the convection zone $d = (r_o - r_t)$, magnetic field by $\lambda_o \sqrt{\rho\mu}/d$ and time by the magnetic diffusion time d^2/λ_o of the convection zone. Similar to the cartesian dynamo model discussed in the previous section, we can also derive the four sets of dimensionless equations for the four zones (all variables in the rest of the section are non-dimensional)

$$\frac{\partial \mathbf{B}_i}{\partial t} + \beta_i \nabla \times \nabla \times \mathbf{B}_i = 0, \quad 0 < r < r_i, \tag{3.1}$$

$$\nabla \cdot \mathbf{B}_i = 0, \quad 0 < r < r_i; \tag{3.2}$$

$$\frac{\partial \mathbf{B}_t}{\partial t} = R_m \nabla \times \{[\Omega_t(r, \theta) \mathbf{k} \times \mathbf{r}] \times \mathbf{B}_t\} - \beta_t \nabla \times \nabla \times \mathbf{B}_t, \quad r_i < r < r_t, \tag{3.3}$$

$$\nabla \cdot \mathbf{B}_t = 0, \quad r_i < r < r_t; \tag{3.4}$$

$$\frac{\partial \mathbf{u}}{\partial t} + \mathbf{u} \cdot \nabla \mathbf{u} + P_m Ta^{1/2} \mathbf{k} \times \mathbf{u} = -\nabla p + (\nabla \times \mathbf{B}_o) \times \mathbf{B}_o + P_m \nabla^2 \mathbf{u}, \quad r_t < r < r_o, \tag{3.5}$$

$$\nabla \cdot \mathbf{u} = 0, \quad r_t < r < r_o, \tag{3.6}$$

$$\frac{\partial \mathbf{B}_o}{\partial t} = R_\alpha \nabla \times [\alpha(r, \theta, \phi, |\mathbf{B}_o|^2) \mathbf{B}_o] + \nabla \times (\mathbf{u} \times \mathbf{B}_o) - \nabla \times \nabla \times \mathbf{B}_o, \quad r_t < r < r_o, \tag{3.7}$$

$$\nabla \cdot \mathbf{B}_o = 0, \quad r_t < r < r_o; \tag{3.8}$$

$$\frac{\partial \mathbf{B}_e}{\partial t} + \beta_m \nabla \times \nabla \times \mathbf{B}_e = 0, \quad r_o < r \leq r_m, \tag{3.9}$$

$$\nabla \cdot \mathbf{B}_e = 0, \quad r_o < r \leq r_m. \tag{3.10}$$

There are seven non-dimensional quantities that characterize the dynamic interface dynamo: the three magnetic diffusivity ratios β_i , β_t and β_m , the magnetic alpha Reynolds number R_α , the magnetic omega Reynolds number R_m , the magnetic Prandtl number P_m and the Taylor number Ta , which are defined by

$$\beta_i = \frac{\lambda_i}{\lambda_o}, \quad \beta_t = \frac{\lambda_t}{\lambda_o}, \quad \beta_m = \frac{\lambda_e}{\lambda_o},$$

$$R_\alpha = \frac{d\alpha_0}{\lambda_o}, \quad R_m = \frac{d^2|\mathbf{\Omega}|}{\lambda_o}, \quad P_m = \frac{\nu_o}{\lambda_o}, \quad Ta = \left(\frac{2d^2|\mathbf{\Omega}|}{\nu_o}\right)^2.$$

Our numerical simulations have focused on the fixed Taylor number $Ta = 10^5$, which is appropriate for the solar convection zone if taking an eddy viscosity, and a unity magnetic Prandtl number $P_m = 1$ with the magnetic diffusivity ratios at $\beta_i = \beta_t = 0.1$.

The four sets of equations are solved subject to a number of matching and boundary conditions at the interfaces. At the three interfaces of the four zones, $r = r_i, r_t$ and r_o , all components of the magnetic field and the tangential component of the electrical field must be continuous, which yield

$$\begin{aligned} (\mathbf{B}_i - \mathbf{B}_t) &= 0 \text{ at } r = r_i; \\ \mathbf{r} \times (\beta_i \nabla \times \mathbf{B}_i - \beta_t \nabla \times \mathbf{B}_t) &= 0 \text{ at } r = r_i; \\ (\mathbf{B}_t - \mathbf{B}_o) &= 0 \text{ at } r = r_t; \\ \mathbf{r} \times (-\beta_t \nabla \times \mathbf{B}_t - R_\alpha \alpha \mathbf{B}_o + \nabla \times \mathbf{B}_o) &= 0 \text{ at } r = r_t; \\ (\mathbf{B}_e - \mathbf{B}_o) &= 0 \text{ at } r = r_o; \\ \mathbf{r} \times (\beta_m \nabla \times \mathbf{B}_e + R_\alpha \alpha \mathbf{B}_o - \nabla \times \mathbf{B}_o) &= 0 \text{ at } r = r_o. \end{aligned} \tag{3.11}$$

For the boundary condition at the outer bounding surface of the dynamo solution domain (see Figure 3), $r = r_m$, an approximation must be made. Since there are no sources at infinity, i.e.,

$$\mathbf{B}_e = O(r^{-3}), \quad \text{as } r \rightarrow \infty, \tag{3.12}$$

we can approximate the magnetic field boundary condition at $r = r_m$ as

$$\mathbf{B}_e = 0 \quad \text{at } r = r_m \quad \text{with } (r_m/r_o)^3 \gg 1. \tag{3.13}$$

Equations (3.1-3.10) together with the matching and boundary conditions (3.11)-(3.13), define a nonlinear dynamic interface dynamo problem in a multilayered spherical rotating systems.

For given parameters of the dynamo model like R_α and R_m , nonlinear solutions of the dynamic interface dynamo are obtained by performing fully three-dimensional simulations on massively parallel computers. Figure 4 shows contours of the toroidal magnetic field at the interface r_t , the radial magnetic field and the toroidal flow at the middle of the convection zone, plotted against time, for $R_m = 200$, revealing the typical properties of the dynamic interface dynamos for sufficiently large magnetic Reynolds number R_m . We find, with the strong effect of the tachocline for $R_m \geq O(10)$, that (i) the action of the strong tachocline always produces an oscillatory dynamic dynamo with a period of about two magnetic diffusion units, (ii) the multilayered dynamic interface dynamos also produce a torsional oscillation of the azimuthal flow with a period of about one magnetic diffusion unit, (iii) the dynamic dynamo is usually axisymmetric, selects dipolar symmetry and propagates equatorward though the simulation is fully three-dimensional and (iv) the generated magnetic field mainly concentrates in the vicinity of the interface between the tachocline and the convection zone.

4. Remarks

We have followed the idea of Parker’s interface dynamo by separating the alpha and omega processes spatially, an essential ingredient in any interface dynamos, in both the cartesian and spherical multilayered interface dynamos consisting of four regions coupled magnetically through the matching conditions at the interfaces. It is of importance to note

that, in the multilayered interface dynamos discussed, the shear flow in the tachocline is imposed and the complicated problem of thermal convection (see, for example, Brun and Toomre, 2002) is avoided.

The most formidable difficulty in modelling the solar global magnetic fields such as the 22-year solar cycle and the polarity rules is perhaps related to the questions why and how the solar tachocline is formed and confined at the top of the radiative core and how to treat the solar radiative core in the solar dynamo simulations (Zhang and Schubert, 2006). Understanding the formation and confinement of the tachocline represents a key prerequisite in understanding the global properties of the solar dynamo. We must consider three major zones of the Sun, the nearly solid-body rotating core, the tachocline and the turbulent convection zone, as a single dynamically coupled magnetic system. A sufficiently strong magnetic field in the core, which may be primordial or diffused into the core from the above (Garaud, 2002), is needed to sustain dynamically the solid-body rotation of the core (Gough & McIntyre, 1998). It remains a great challenge that an interface dynamo model, containing the three major zones of the Sun, is capable of producing the formation and confinement of the tachocline in a dynamically self-consistent way.

Acknowledgements

XL is supported by NSFC grant/10633030 and KZ is supported by UK NERC and PPARC grants. Computation is supported by Shanghai Supercomputer Center.

References

- Brandenburg, A., Krause, F., Meinel, R., Moss, D., & Tuominen, I. 1989, *Astronomy and Astrophysics*, 213, 411
- Brown, T.M., Christensen-Dalsgaard, J., Dziembowski, W.A., Goode, P., Gough, D.O., and Morrow, C.A. *Astrophys. J.*, 1989, 343, 526
- Brun, A.S. & Toomre, J. 2002, *Astrophys. J.*, 570, 865
- Bushby, P. J. 2003, *MNRAS*, 342, L15
- Chan, K. H., X. Liao, Zhang K. and Jones C.A., 2004, *Astron. Astrophys.*, 423, L37.
- Chan, K. H., Zhang, K., Li, L., & Liao, X. 2007, *Phys. Earth Planet. Inter.*, 163, 251
- Charbonneau, P., & MacGregor, K. B. 1997, *Astrophys. J.*, 486, 502
- Dikpati, M., & Charbonneau, P. 1999, *Astrophys. J.*, 518, 508
- Garaud, P., 2002, *MNRAS*, 329, 1
- Gough, D. O., & McIntyre, M. E. 1998, *Nature*, 394, 755
- Hoyt, D.V. and Schatten K.H. 1997, *The role of the Sun in climate change* Oxford University Press.
- MacGregor, K. B., & Charbonneau, P. 1997, *Astrophys. J.*, 486, 484
- Markiel, J. A., & Thomas, J. H. 1999, *Astrophys. J.*, 523, 827
- Parker, E. N. 1993, *Astrophys. J.*, 408, 707
- Ponty, Y., Gilbert, A., & Soward, A. M. 2001, *J. Fluid Mech.*, 435, 261
- Schou, J., *et al.* 1998, *Astrophys. J.*, 505, 390
- Spiegel, E. A., & Zahn, J.-P. 1992, *A & A*, 265, 106
- Tobias, S. M. 1997, *Geophys. Astrophys. Fluid Dynamics*, 86, 287
- Zhang K., Chan K. H., Zou J., Liao X. and Schubert G. 2003 *Astrophys. J.*, 596, 663
- Zhang, K., Liao X., and Schubert G., 2004, *Astrophys. J.*, 602, 468
- Zhang, K. and Schubert G., 2006, *Rep. Prog. Phys.* 69, 1581.